JOURNAL OF GUIDANCE, CONTROL, AND DYNAMICS
Vol. 16, No. 1, January–February 1993

Innovative Approach to the Momentum Management Control for Space Station Freedom

Jalal Mapar*
Grumman Space Station Integration Division, Reston, Virginia 22090

A new approach to the control moment gyro (CMG) momentum management and attitude control of the Space Station Freedom is presented. First, the nonlinear equations of motion are developed in terms of body attitude and attitude rate with respect to the local horizontal local vertical (LVLH); then, they are linearized about any arbitrary stable point via the use of perturbation techniques. It is shown that, for some assembly flights, linearization of the equations of motion about the LVLH may not be valid and that a better choice would be to linearize about a torque equilibrium attitude (TEA). Next, a three-axis-coupled control law is used and the controller gains are determined via a combination of the optimal control and regional pole placement techniques. Finally, it is shown that the proposed linearization process, together with the coupled control laws, can stabilize a previously uncontrollable space station assembly flight.

Introduction

THE Space Station Freedom will require several Space Shuttle flights to complete. When activated after a few assembly flights, it will use CMGs as the primary attitude control devices during normal flight operations. Since CMGs are momentum exchange devices, external torques must be applied to prevent momentum saturation. Several momentum management methods, both discrete and continuous, have been developed.[1-6] These methods are based on the use of environmental torques to drive the vehicle to a TEA, thus minimizing CMG momentum usage.

In all previous work, the space station equations of motion (EOM) have been linearized about the LVLH. It is assumed that the products of inertia remain small, i.e., principal axes nearly aligned with the LVLH, allowing the pitch axis to be decoupled while the roll/yaw axes remain coupled. These assumptions are used by Wie et al.[3] in the development of a continuous momentum management system (MMS) that uses the linear quadratic regulator (LQR) technique for generating feedback gains. The continuous MMS, as proposed by Wie et al.,[3] is represented in simple block diagram form in Fig. 1. The weighting matrices associated with the LQR are obtained by trial and error. This process is often time consuming and does not always yield desirable closed-loop poles.

More recently, Warren et al.[4] have presented the EOM for the case of large pitch TEA, which may be encountered during the assembly flights of the space station, but, in order to simplify the equations, they have neglected the products of inertia. Since the large TEAs are chiefly due to large products of inertia, the applicability of the equations to early stages of the station is debatable. However, when applied to the assembly complete vehicle, the controller, which also includes disturbance rejection filters to minimize the steady-state effects of the aerodynamic torques, is shown to stabilize the system by achieving the TEA. Sunkel and Shieh[5] have applied the regional pole placement and optimal control techniques to the linearized model of the space station and have solved directly for both the feedback gains and the weighting matrices. They use the matrix sign function algorithm for the solution of the Riccati equations and show drastic time savings associated with the manual assignment of the weighting matrices, as used by Wie et al.[3,4] Again, the momentum management algorithm is applied to the assembly complete vehicle, and stability is obtained as before.

Although the simplifying assumptions used in previous studies[1-6] are valid for assembly complete-type space station configurations, they may not be applicable for the buildup stages. Holmes[7] has applied the momentum management algorithm developed by Wie et al.[3,4] to one of the station assembly flights and has shown that the large products of inertia produce a large TEA, thus invalidating the assumptions used in the previous studies.[1-6]

This paper presents a new approach to modeling the rigid body dynamics by developing the EOM and linearizing them about any arbitrary point along the attitude trajectory. A suitable stable point is proposed for linearization of the EOM. It is shown that a three-axis-coupled control law, whose gains are determined by regional pole placement,[5] can successfully stabilize an assembly flight that was not previously controllable. The proposed momentum management method is given in its generic form so that it can be easily applied to the assembly complete-type configurations as a special case. Finally, a comparison is made between the proposed method and the

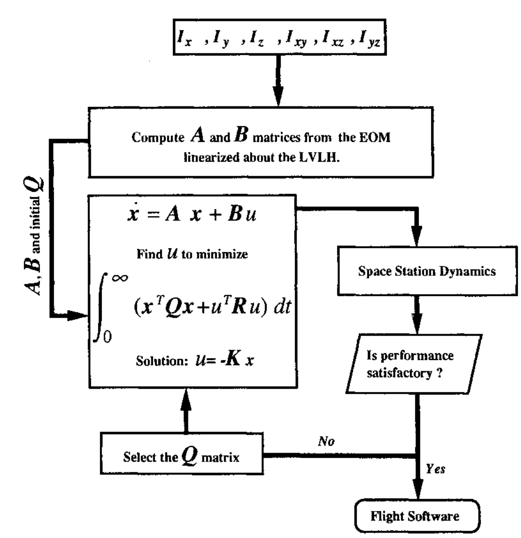

Fig. 1 Simple block diagram of the MMS after Wie et al.[3]

Presented as Paper 90-3317 at the AIAA Guidance, Navigation, and Control Conference, Portland, OR, Aug. 20–22, 1990; received June 7, 1991; revision received Feb. 14, 1992; accepted for publication March 5, 1992.

*Manager, Flight Mechanics, 1760 Business Center Drive. Senior Member AIAA.

previous algorithms by presenting simulation results for a space station assembly vehicle.

Mathematical Models

In this section the rotational EOM are presented in matrix form and linearized about any arbitrary point. Next, a suitable stable point is proposed for linearization, and the EOM are simplified. For simplicity, the station is assumed to be a single rigid body in a circular orbit. The nonlinear rotational EOM in terms of components along the fixed body-axes are given by the well-known Euler's equations:

$$I\dot{\omega} + \tilde{\omega} I \omega = T_{nc} + u \tag{1}$$

Here, the $\tilde{}$ represents the skew symmetric matrix and

$$\tilde{\omega} = \begin{bmatrix} 0 & -\omega_z & \omega_y \\ \omega_z & 0 & -\omega \\ -\omega_y & \omega_x & 0 \end{bmatrix}, \qquad I = \begin{bmatrix} I_x & I_{xy} & I_{xz} \\ I_{xy} & I_y & I_{yz} \\ I_{xz} & I_{yz} & I_z \end{bmatrix}$$

where $(\omega_x, \omega_y, \omega_z)$ are the body-axis components of the angular rate with respect to the inertial frame; (I_x, I_y, I_z) the moments inertia and (I_{xy}, I_{xz}, I_{yz}) the products of inertia; and $(\dot{\cdot})$ the time derivative. The noncontrol torque T_{nc} is the sum of the gravity gradient and aerodynamic torques, which will be given later, and u is the control torque, which is related to the CMG momentum, H by

$$\dot{H} + \tilde{\omega} H = -u \tag{2}$$

The body rate can be expressed as

$$\omega = \omega_{B/L} + \omega_L \tag{3}$$

where $\omega_{B/L}$ is the body rate vector with respect to LVLH and ω_L the LVLH rate vector in the body-axes. For a pitch-yaw-roll (2-3-1) Euler rotation sequence, $\omega_{B/L}$ and ω_L are given by[8]

$$\omega_{B/L} = \begin{bmatrix} \dot{\phi} + \dot{\theta}\, S\psi \\ \dot{\theta}\, C\phi\, C\psi + \dot{\psi}\, S\phi \\ -\dot{\theta}\, S\phi\, C\psi + \dot{\psi}\, C\phi \end{bmatrix} \tag{3a}$$

and

$$\omega_L = \begin{bmatrix} -n\, S\psi \\ -n\, C\phi\, C\psi \\ n\, S\phi\, C\psi \end{bmatrix} \tag{3b}$$

where $C = \cos$ and $S = \sin$; ϕ, θ, and ψ the body attitude with respect to the LVLH; and n the orbital rate.

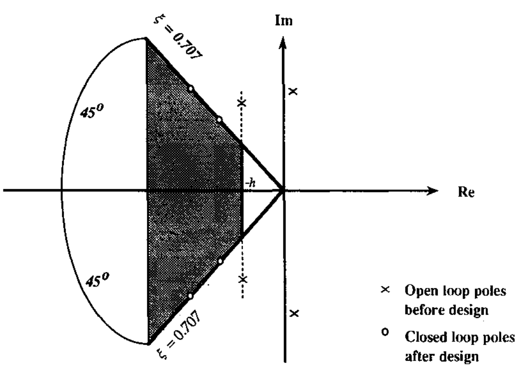

Fig. 2 Pole assignment sector.

Equations (3a) and (3b) can be used to express the total body rate as

$$\omega = F\dot{\Phi} + G \tag{4}$$

where

$$F = \begin{bmatrix} 1 & S\psi & 0 \\ 0 & C\phi\, C\psi & S\phi \\ 0 & -S\phi\, C\psi & C\phi \end{bmatrix} \tag{4a}$$

$$G = \begin{bmatrix} -n\, S\psi \\ -n\, C\phi\, C\psi \\ n\, S\phi\, C\psi \end{bmatrix} \tag{4b}$$

and Φ represents the roll, pitch, and yaw attitude angles with respect to LVLH.

$$\Phi = \begin{bmatrix} \phi \\ \theta \\ \psi \end{bmatrix} \tag{4c}$$

Note that the total body rate is now expressed in terms of F and G, which are functions of the attitude and attitude rate with respect to LVLH and orbit rate. Equation (4) can be differentiated to give the body angular acceleration as

$$\dot{\omega} = F\ddot{\Phi} + \dot{F}\dot{\Phi} + \dot{G} \tag{5}$$

where

$$\dot{F} = \begin{bmatrix} 0 & \dot{\psi} C\psi & 0 \\ 0 & -\dot{\phi}\, S\phi\, C\psi - \dot{\psi}\, C\phi\, S\psi & \dot{\phi} C\phi \\ 0 & -\dot{\phi}\, C\phi\, C\psi + \dot{\psi}\, S\phi\, S\psi & -\dot{\phi} S\phi \end{bmatrix} \tag{5a}$$

Substituting Eqs. (4) and (5) into Eq. (1) and simplifying yields

$$\ddot{\Phi} = (IF)^{-1}\{T_{nc} - (\widetilde{F\dot{\Phi} + G})I(F\dot{\Phi} + G)\} - F^{-1}(\dot{F}\dot{\Phi} + \dot{G}) + (IF)^{-1}u \tag{6}$$

Equation (6) represents the nonlinear rotational dynamics of a body with respect to the rotating LVLH coordinate system. By integrating Eq. (6), one can obtain both the body attitude and the attitude rate with respect to LVLH directly. Note that in Eq. (6) no assumption on the products of inertia has been introduced.

The gravity gradient torque T_{gg} is given by

$$T_{gg} = 3n^2 \tilde{R} I R \tag{7}$$

where R is the unit vector from the center of Earth to the center of mass of the vehicle. For a (2-3-1) rotation sequence, R can be expressed as

$$R = \begin{bmatrix} S\theta\, C\psi \\ -S\phi\, C\theta - C\phi\, S\theta\, S\psi \\ -C\phi\, C\theta + S\phi\, S\theta\, S\psi \end{bmatrix} \tag{8}$$

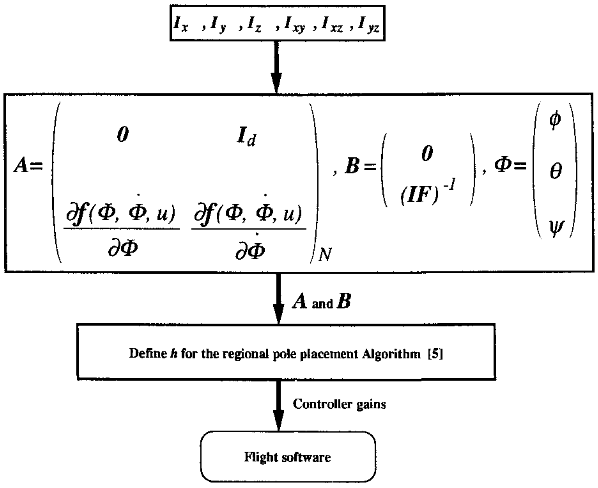

Fig. 3 Simple block diagram of the proposed MMS.

The aerodynamic torque is modeled as bias plus cyclic terms[3-5] in the body axes as

$$T_{\text{aero}} = \text{Bias} + \sum_{k=1}^{m} A_k \sin(knt + \varphi_k) \tag{9}$$

where, usually, $m = 2$. The cyclic components at once and twice the orbital rate are due to the diurnal bulge effect and the rotating solar panels, respectively. Substituting Eqs. (7) and (9) into Eq. (6) and rewriting the EOM in a more compact functional form yields

$$\ddot{\Phi} = f(\Phi, \dot{\Phi}, u) \tag{10}$$

Because the expansion of EOM will result in rather lengthy expressions, we will proceed with the matrix notation until the final result is obtained. Equation (10) represents the most general form of the nonlinear EOM in terms of the body attitude and rate with respect to LVLH. Linearization of the EOM is performed by applying small perturbations to the nominal solution of Eq. (10). Let $\Phi_N(t)$ be such a nominal solution. Then, for small perturbations from a point on the nominal trajectory, the solution of Eq. (10), to first order, is given by

$$\begin{aligned} \Phi(t) &\cong \Phi_N(t) + \delta\Phi(t) \\ \dot{\Phi}(t) &\cong \dot{\Phi}_N(t) + \delta\dot{\Phi}(t) \end{aligned} \tag{11}$$

where $\delta\Phi(t)$ represents any small perturbation from the nominal trajectory. Applying Eq. (11) to Eq. (10), and noting that $\delta\Phi(t)$ would give rise to a perturbation in u, will yield the desired linearized EOM:

$$\delta\ddot{\Phi} = \left\{\frac{\partial f(\Phi, \dot{\Phi}, u)}{\partial \Phi}\right\}_N \delta\Phi + \left\{\frac{\partial f(\Phi, \dot{\Phi}, u)}{\partial \dot{\Phi}}\right\}_N \delta\dot{\Phi} + \left\{\frac{\partial f(\Phi, \dot{\Phi}, u)}{\partial u}\right\}_N \delta u \tag{12}$$

where the subscript N means "at the nominal point." Equation (12) can be written in first order form as

$$\delta\dot{x} = A\ \delta x + B\ \delta u \tag{13}$$

where

$$\delta x = \begin{bmatrix} \delta\Phi \\ \delta\dot{\Phi} \end{bmatrix}, \qquad \delta u = \begin{bmatrix} \delta u_x \\ \delta u_y \\ \delta u_z \end{bmatrix} \tag{13a}$$

$$A = \begin{bmatrix} 0 & I_d \\ \dfrac{\partial f}{\partial \Phi} & \dfrac{\partial f}{\partial \dot{\Phi}} \end{bmatrix}_N, \qquad B = \begin{bmatrix} 0 \\ (IF)^{-1} \end{bmatrix} \tag{13b}$$

and I_d is a 3×3 identity matrix. Equation (13) represents the new linearized EOM about any arbitrary point. By defining a nominal stable path, i.e., a nominal attitude and rate, the A and B matrices can be evaluated. Note that the A matrix is now a function of the attitude and attitude rate. In order to simplify the A matrix, we propose that the nominal point be an estimate of the TEA. If an accurate estimate of the TEA may not be available initially, it is proposed that, as a first choice, the estimated TEA be the principal-to-body Euler angles, ϕ_p, θ_p, and ψ_p, which are easily determined from the vehicle inertia matrix. Furthermore, it is recognized that at the TEA the vehicle attitude rates will be negligible, thus, allowing the A matrix to be a function of the inertia, the estimated TEA, and orbit rate.

Since, at the estimated TEA, the nominal values of H and u are expected to be zero, the perturbation equations for the CMG momentum are

$$\delta\dot{H} + \tilde{\omega}_N\ \delta H = -\delta u \tag{14}$$

where $\tilde{\omega}_N$ is evaluated from Eq. (4) by setting

$$\phi = \phi_p, \qquad \theta = \theta_p, \qquad \psi = \psi_p \tag{15}$$

It can be easily shown that the EOM as used before[3-5], i.e., EOM linearized about the LVLH, become a special case of the new linearized equations previously presented simply by setting

$$\phi_p = \theta_p = \psi_p = 0, \qquad I_{xy} = I_{xz} = I_{yz} = 0$$

in the A and B matrices as given by Eq. (13a). The A and B matrices are given in the Appendix. The state-space representation in Eqs. (13) and (14) is the most general form of the three-axis-coupled EOM linearized about any arbitrary point and forms the basis of the momentum management algorithm, which is discussed in detail in the next section.

Momentum Management System

In this section the proposed MMS is described, a three-axis-coupled control law is presented, and evaluation of the controller gains through the use of the regional pole placement technique is discussed briefly. The MMS algorithm is based on the new linearized EOM as given by Eqs. (13) and (14). The concept of linearizing the EOM about the principal-to-body angles allows us to treat the aerodynamic torques as a perturbation from the nominal TEA trajectory. In the absence of aerodynamic torques, the TEA is simply the principal-to-body Euler angles. The effect of the aerodynamic torque can then be superimposed on this initial TEA solution, and the problem can be considered as a perturbation feedback control in the vicinity of an estimated TEA. Since the EOM are developed in terms of attitude and attitude rate with respect to LVLH, and the coupling has resulted from the inclusion of the products of

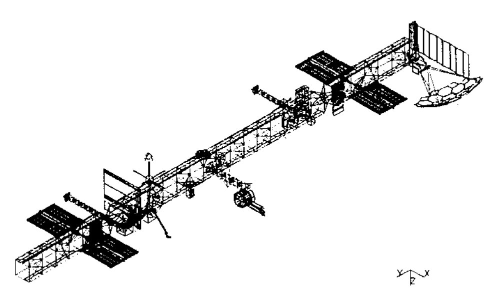

Fig. 4 A representative assembly flight no. 5.

Table 1 Vehicle parameters

Inertia, slugs-ft^2		Aerodynamic torque, ft-lbs	
I_x	3.9676E7	Roll	$-0.2 + 0.1\sin(nt) + 0.01\sin(2nt)$
I_y	2.5588E6	Pitch	$1.2 + 0.4\sin(nt) + 0.1\sin(2nt)$
I_z	4.544E7	Yaw	$-1.0 + 0.8\sin(nt) + 0.2\sin(2nt)$
I_{xy}	−1.5544E6		
I_{xz}	2.6162E5		
I_{yz}	−2.6641E5		

Table 2 Controller gains for the proposed MMS

Gain	Roll	Pitch	Yaw
K_ϕ	−3.9955E + 03	2.4912E + 02	−7.4628E + 03
$K_{\dot\phi}$	−7.0403E + 06	2.9447E + 05	−2.2441E + 06
K_{H_x}	−1.5960E − 01	3.9543E − 03	−5.5844E − 02
$K_{\hat H_x}$	2.1858E − 05	−1.1165E − 06	−2.6547E − 05
K_{α_1}	−7.1639E − 08	2.1939E − 09	4.9216E − 08
$K_{\dot\alpha_1}$	−5.3398E − 05	2.4520E − 06	−1.8211E − 05
K_{β_1}	−2.4546E − 08	1.1314E − 09	−4.0185E − 09
$K_{\dot\beta_1}$	−6.4831E − 05	3.0419E − 06	−5.1983E − 05
K_θ	−2.2744E + 01	−2.9607E + 02	−1.0508E + 01
$K_{\dot\theta}$	3.3452E + 02	−2.1455E + 05	−7.9875E + 03
K_{H_y}	6.3739E − 03	−7.0746E − 02	3.5599E − 05
$K_{\hat H_y}$	−1.5117E − 06	−1.4176E − 05	8.6180E − 07
K_{α_2}	5.9816E − 06	−7.3818E − 05	4.6329E − 06
$K_{\dot\alpha_2}$	−2.9465E − 02	−3.0523E − 01	9.3062E − 03
K_{β_2}	6.3893E − 06	−7.7034E − 04	3.0838E − 05
$K_{\dot\beta_2}$	−1.3276E − 02	−2.6569E − 01	−3.8467E − 03
K_ψ	8.5886E + 03	−3.3449E + 02	−1.3101E + 03
$K_{\dot\psi}$	5.5514E + 06	−1.7698E + 05	−2.8710E + 06
K_{H_z}	1.3843E − 01	−5.0197E − 03	−5.5323E − 02
$K_{\hat H_z}$	2.3378E − 05	−1.0742E − 06	7.0517E − 06
K_{α_3}	5.6120E − 03	−2.1757E − 04	7.2290E − 04
$K_{\dot\alpha_3}$	2.4630E + 00	−6.8696E − 02	−3.5602E + 00
K_{β_3}	7.9672E − 03	−2.2645E − 04	−8.4278E − 03
$K_{\dot\beta_3}$	1.8513E − 02	3.0751E − 02	−4.6049E + 00

inertia, we use a three-axis-coupled control law for each axis as follows:

$$\begin{aligned}\delta u_x = {} & K^1_\phi\delta\phi + K^1_{\dot\phi}\delta\dot\phi + K^1_{H_x} + \delta H_x + K^1_{\hat H_x}\delta\hat H_x + K^1_{\alpha_1}\alpha_1 \\ & + K^1_{\dot\alpha_1}\dot\alpha_1 + K^1_{\beta_1}\beta_1 + K^1_{\dot\beta_1}\dot\beta_1 + K^1_\theta\delta\theta + K^1_{\dot\phi}\delta\dot\theta + K^1_{H_y}\delta H_y \\ & + K^1_{\hat H_y}\delta\hat H_y + K^1_{\alpha_2}\alpha_2 + K^1_{\dot\alpha_2}\dot\alpha_2 + K^1_{\beta_2}\beta_2 + K^1_{\dot\beta_2}\dot\beta_2 + K^1_\psi\delta\psi \\ & + K^1_{\dot\psi}\delta\dot\psi + K^1_{H_z}\delta H_z + K^1_{\hat H_z}\delta\hat H_z + K^1_{\alpha_3}\alpha_3 + K^1_{\dot\alpha_3}\dot\alpha_3 \\ & + K^1_{\beta_3}\beta_3 + K^1_{\dot\beta_3}\dot\beta_3\end{aligned} \tag{16a}$$

$$\begin{aligned}\delta u_y = {} & K^2_\phi\delta\phi + K^2_{\dot\phi}\delta\dot\phi + K^2_{H_x} + \delta H_x + K^2_{\hat H_x}\delta\hat H_x + K^2_{\alpha_1}\alpha_1 \\ & + K^2_{\dot\alpha_1}\dot\alpha_1 + K^2_{\beta_1}\beta_1 + K^2_{\dot\beta_1}\dot\beta_1 + K^2_\theta\delta\theta + K^2_{\dot\phi}\delta\dot\theta + K^2_{H_y}\delta H_y \\ & + K^2_{\hat H_y}\delta\hat H_y + K^2_{\alpha_2}\alpha_2 + K^2_{\dot\alpha_2}\dot\alpha_2 + K^2_{\beta_2}\beta_2 + K^2_{\dot\beta_2}\dot\beta_2 + K^2_\psi\delta\psi \\ & + K^2_{\dot\psi}\delta\dot\psi + K^2_{H_z}\delta H_z + K^2_{\hat H_z}\delta\hat H_z + K^2_{\alpha_3}\alpha_3 + K^2_{\dot\alpha_3}\dot\alpha_3 \\ & + K^2_{\beta_3}\beta_3 + K^2_{\dot\beta_3}\dot\beta_3\end{aligned} \tag{16b}$$

$$\begin{aligned}\delta u_z = {} & K^3_\phi\delta\phi + K^3_{\dot\phi}\delta\dot\phi + K^3_{H_x} + \delta H_x + K^3_{\hat H_x}\delta\hat H_x + K^3_{\alpha_1}\alpha_1 \\ & + K^3_{\dot\alpha_1}\dot\alpha_1 + K^3_{\beta_1}\beta_1 + K^3_{\dot\beta_1}\dot\beta_1 + K^3_\theta\delta\theta + K^3_{\dot\theta}\delta\dot\theta + K^3_{H_y}\delta H_y \\ & + K^3_{\hat H_y}\delta\hat H_y + K^3_{\alpha_2}\alpha_2 + K^3_{\dot\alpha_2}\dot\alpha_2 + K^3_{\beta_2}\beta_2 + K^3_{\dot\beta_2}\dot\beta_2 + K^3_\psi\delta\psi \\ & + K^3_{\dot\psi}\delta\dot\psi + K^3_{H_z}\delta H_z + K^3_{\hat H_z}\delta\hat H_z + K^3_{\alpha_3}\alpha_3 + K^3_{\dot\alpha_3}\dot\alpha_3 \\ & + K^3_{\beta_3}\beta_3 + K^3_{\dot\beta_3}\dot\beta_3\end{aligned} \tag{16c}$$

where the gain superscripts (1, 2, 3) refer to the roll, pitch, and yaw axes. In order to avoid CMG momentum buildup, we have included the integral of the CMG momentum vector $\boldsymbol{H}$, i.e.,

$$\delta\hat{\boldsymbol{H}} = \int \delta\boldsymbol{H}\,\mathrm{d}t \qquad \text{or} \qquad \delta\dot{\hat{\boldsymbol{H}}} = \delta\boldsymbol{H} \tag{17}$$

Note that, in order to minimize the steady-state oscillations of roll, pitch, yaw attitude, and CMG momentum, we have used the cyclic disturbance rejection filters as proposed by Wie et al.[3] The filter equations are given as follows for momentum rejection in roll and for attitude rejection in pitch and yaw at frequencies n and $2n$:

$$\ddot\alpha_1 + (n)^2\alpha_1 = \delta H_x \tag{18a}$$

$$\ddot\beta_1 + (2n)^2\beta_1 = \delta H_x \tag{18b}$$

$$\ddot\alpha_2 + (n)^2\alpha_2 = \delta\theta \tag{19a}$$

$$\ddot\beta_2 + (2n)^2\beta_2 = \delta\theta \tag{19b}$$

$$\ddot\alpha_3 + (n)^2\alpha_3 = \delta\psi \tag{20a}$$

$$\ddot\beta_3 + (2n)^2\beta_3 = \delta\psi \tag{20b}$$

Also, in the control laws we have chosen the attitude rate with respect to LVLH in all three axes. To compute the gains

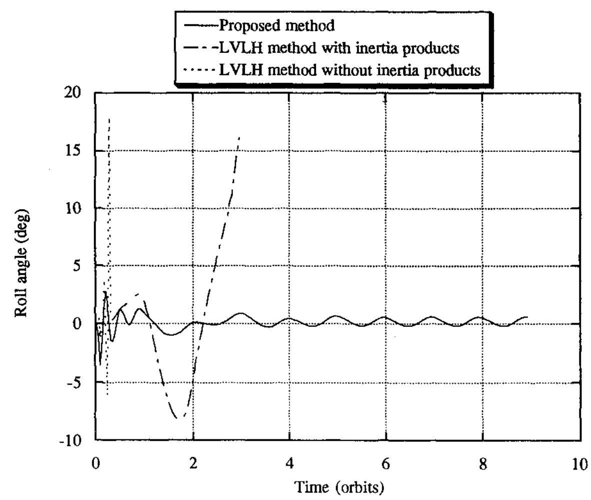

Fig. 5a Roll attitude comparison.

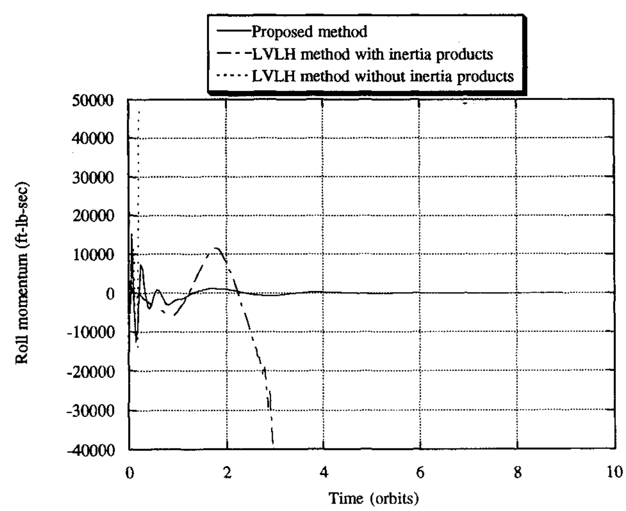

Fig. 5b Roll momentum comparison.

associated with the control laws, we use the LQR with the regional pole placement technique. Let the quadratic performance index for the system in Eq. (13) be

$$J = \int_0^\infty (x^T Q x + u^T R u)\, dt \tag{21}$$

where the weighting matrices Q and R are $n \times n$ non-negative and $m \times m$ positive definite symmetric matrices, respectively. The feedback control law that minimizes the performance index in Eq. (21) is given by

$$u = -Kx = R^{-1}B^T P x \tag{22}$$

where K is the feedback gain and P, an $n \times n$ non-negative definite symmetric matrix, the solution of the Riccati equation

$$PBR^{-1}B^T P - PA - A^T P - Q = 0 \tag{23}$$

The regional pole placement used to generate the feedback gains in Eq. (16) is adapted from the algorithm by Sunkel and Shieh.[5] They solve for Q, R, and K so that the closed-loop system $(A\text{-}BK)$ has eigenvalues on or within a specified region, as shown in Fig. 2, without explicitly using the eigenvalues of the open-loop system. The process involves the use of matrix sign function techniques for the solution of the modified Riccati Eq. (23). It is shown in Ref. 5 that the use of the matrix sign function greatly reduces the computational time required

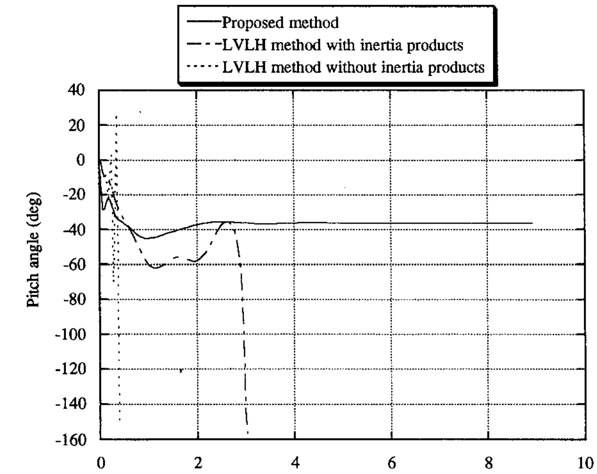

Fig. 6a Pitch attitude comparison.

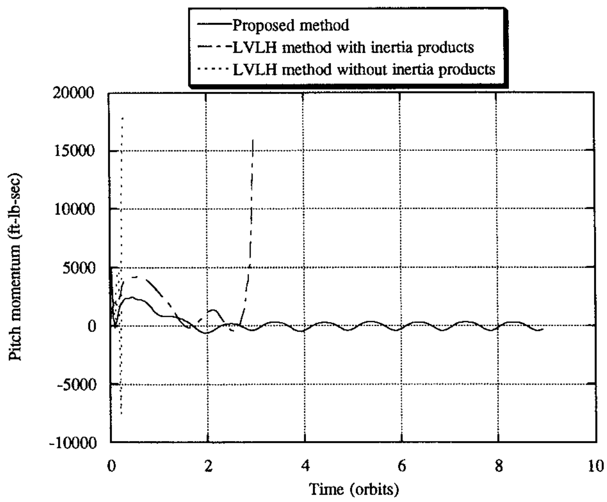

Fig. 6b Pitch momentum comparison.

Table 3 Controller gains for MMS with the products of inertia

Gain	Roll	Pitch	Yaw
K_ϕ	−6.3782E + 03	−1.1138E + 03	−7.2501E + 03
$K_{\dot\phi}$	−7.4340E + 06	−5.5993E + 04	−2.8623E + 06
K_{H_x}	−1.7086E − 01	−4.5833E − 03	−6.9965E − 02
$K_{\dot H_x}$	2.0660E − 05	−5.6989E − 06	−2.1460E − 05
K_{α_1}	−6.3059E − 08	9.4754E − 09	3.4501E − 08
$K_{\dot\alpha_1}$	−6.5435E − 05	−5.5723E − 06	−2.4424E − 05
K_{β_1}	−1.4985E − 08	−8.2626E − 09	−2.6358E − 08
$K_{\dot\beta_1}$	−5.2853E − 05	−4.9874E − 06	−6.0769E − 05
K_θ	1.6184E + 02	−2.4512E + 02	2.8314E + 02
$K_{\dot\theta}$	2.0548E + 05	−2.1178E + 05	1.7038E + 05
K_{H_y}	−2.6379E − 02	−7.1772E − 02	1.9372E − 02
$K_{\dot H_y}$	−4.1007E − 06	−1.4227E − 05	3.6292E − 06
K_{α_2}	6.0585E − 05	−5.0400E − 05	4.0185E − 05
$K_{\dot\alpha_2}$	1.0943E − 01	−2.8673E − 01	2.9582E − 02
K_{β_2}	1.1648E − 04	−7.1040E − 04	1.9887E − 05
$K_{\dot\beta_2}$	3.5338E − 02	−2.7269E − 01	2.9872E − 02
K_ψ	8.5367E + 03	−2.5045E + 02	−8.6827E + 02
$K_{\dot\psi}$	3.0459E + 06	−5.7297E + 05	−1.7326E + 06
K_{H_z}	7.7348E − 02	−1.4295E − 02	−2.6646E − 02
$K_{\dot H_z}$	2.8022E − 05	2.7870E − 07	7.3450E − 06
K_{α_3}	3.6274E − 03	−3.6923E − 04	1.3482E − 03
$K_{\dot\alpha_3}$	5.0831E + 00	−4.5678E − 01	−3.1003E + 00
K_{β_3}	6.6188E − 03	−1.6058E − 03	−8.6147E − 03
$K_{\dot\beta_3}$	1.8543E + 00	−1.6015E − 02	−4.2424E + 00

for the solution of the Riccati equations. The design procedure is given in detail in Ref. 5 and will not be repeated here.

The MMS presented in this article is shown in block diagram form in Fig. 3. The algorithm depends only on an estimate of the inertia properties of the vehicle. The estimated TEA angles are extracted from the principal-to-body axes transformation matrix. The matrix is obtained by simply calculating the eigenvector matrix associated with the inertia matrix. Next, these angles are used to compute A and B. These matrices are then used to generate the gains for the control laws, as given in Eq. (16), via the LQR and regional pole placement.[5] Note that, in contrast to the method shown in Fig. 1, this procedure does not require any trial and error iterations on the weighting matrices and can be easily automated. However, the parameter h may need to be adjusted to achieve the desired system response and robustness.

Results

In this section we present simulation results for a space station assembly flight and compare the proposed MMS with that of Ref. 3. The vehicle under consideration, assembly flight no. 5 (MB-5), is shown in Fig. 4. This vehicle was also used by Holmes[7] to demonstrate the limitations of the linearization techniques for vehicles with large products of inertia. Although the solar dynamic collectors will not be used on the station, the vehicle was used as a test model to check the MMS algorithm. The vehicle properties, together with a representative aerodynamic torque, are given in Table 1. For MB-5, the principal-to-body angles were computed to be

$$\phi_p = -0.4 \text{ deg}, \qquad \theta_p = -17.1 \text{ deg}, \qquad \psi_p = 2.4 \text{ deg}$$

For gain calculation, the parameter h (see Fig. 2) was set at $0.375n$. The gains for the three-axis-coupled controller are given in Table 2. For consistency, we applied the same pole placement method with the same parameters to the A and B matrices obtained from linearizing the EOM about the LVLH and used the three-axis-coupled control laws presented in this paper. The resulting controller gains for this system that included the products of inertia are given in Table 3. Table 4 includes the gains for the system of EOM linearized about the LVLH without the products of inertia. It is noted that this system reduces to the decoupled pitch and coupled roll/yaw case that has been used before.[3-5]

The results, obtained from nonlinear simulations, are presented in Figs. 5–7. For all of the cases, the vehicle was aligned with the LVLH, i.e., zero attitude and attitude rates, and the initial filter states were set equal to zero. The roll, pitch, and yaw attitude histories, Figs. 5a–7a, show that the proposed MMS converges to a TEA of approximately −36 deg in pitch and the CMG momentum, Figs. 5b–7b, remains bounded after about three orbits. Note that, even though the aerodynamic torque has shifted the estimated pitch TEA (principal-to-body pitch angle) by about 19 deg, the controller has stabilized the system. The stability can be attributed to the fact that the linearized EOM about an estimated TEA provide a better representation of the total system dynamics. In contrast, the MMS based on the EOM linearized about LVLH (both including and excluding the products of inertia) does not perform well and diverges quickly. The instability is mainly due to the fact that the $\boldsymbol{A}$ and $\boldsymbol{B}$ matrices, obtained from the EOM linearized about the LVLH, do not adequately describe the dynamics of the system under consideration. As a result, omission of the products of inertia, and the use of small angle approximation, do not appear to be valid assumptions for MB-5 and other stages that follow the same trend on the inertia properties.

The MMS algorithm presented in this paper has been developed such that the only inputs to it are the characteristics of the vehicle to be controlled, i.e, the inertia matrix, and the parameter h for the gain calculation. Since linearization about any arbitrary point is included in Eq. (13), the algorithm can compute the $\boldsymbol{A}$ and $\boldsymbol{B}$ matrices and the controller gains automatically. The total process is computationally fast and can be automated so that the MMS can adapt to any configuration by simply acquiring the minimum amount of information about the system to be controlled.

Table 4 Controller gains for MMS without the products of inertia

Gain	Roll	Pitch	Yaw
K_{ϕ}	−6.2380e+03	0	−7.3462e+03
$K_{\dot{\phi}}$	−7.4670e+06	0	−2.8323e+06
K_{H_x}	−1.7022e−01	0	−7.0260e−02
$K_{\dot{H}_x}$	2.1507e−05	0	−2.2112e−05
K_{α_1}	−6.4334e−08	0	3.5588e−08
$K_{\dot{\alpha}_1}$	−6.5627e−05	0	−2.4777e−05
K_{β_1}	−1.6112e−08	0	−2.7188e−08
$K_{\dot{\beta}_1}$	−5.2370e−05	0	−6.1311e−05
K_{θ}	0	−2.9685e+02	0
$K_{\dot{\theta}}$	0	−2.1445e+05	0
K_{H_y}	0	−7.0499e−02	0
$K_{\dot{H}_y}$	0	−1.4225e−05	0
K_{α_2}	0	−7.3416e−05	0
$K_{\dot{\alpha}_2}$	0	−3.0602e−01	0
K_{β_2}	0	−7.6917e−04	0
$K_{\dot{\beta}_2}$	0	−2.6605e−01	0
K_{ψ}	8.6848e+03	0	−9.2042e+02
$K_{\dot{\psi}}$	3.1591e+06	0	−1.7899e+06
K_{H_z}	7.8934e−02	0	−2.8506e−02
$K_{\dot{H}_z}$	2.7853e−05	0	7.4502e−06
K_{α_3}	3.6394e−03	0	1.3068e−03
$K_{\dot{\alpha}_3}$	5.1488e+00	0	−3.1523e+00
K_{β_3}	6.6882e−03	0	−8.8185e−03
$K_{\dot{\beta}_3}$	1.8968e+00	0	−4.2499e+00

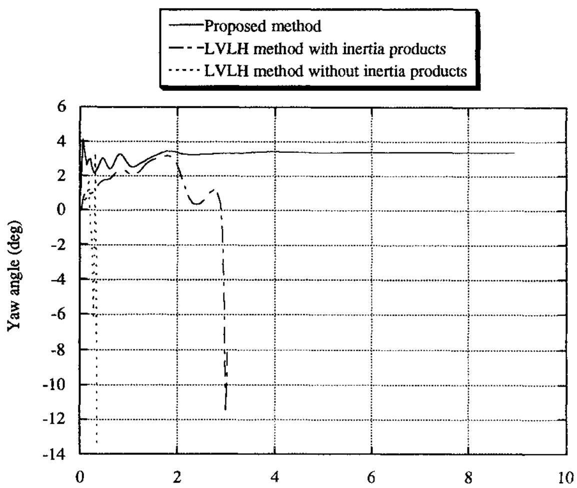

Fig. 7a Yaw attitude comparison.

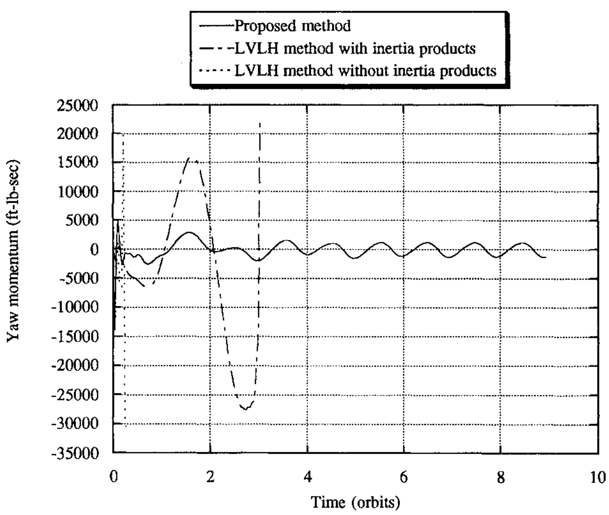

Fig. 7b Yaw momentum comparison.

Conclusions

A new MMS based on linearizing the EOM about an estimated TEA has been presented. A set of three-axis-coupled attitude control laws was also given. It was shown that, for space station vehicles that have strong inertia coupling, the use of small angle approximation and the omission of the products of inertia in the linearized EOM do not provide a good representation of the system dynamics. Although a set of gains can be computed based on linearized models, the use of such models in nonlinear simulations has been shown to destabilize the vehicle.

The proposed MMS is computationally fast and converges quickly. Since the algorithm depends only on the inertia properties and the desired region for the closed-loop system poles, it can adapt to the system if the aforementioned inputs are provided. In fact, depending on the frequency of the gain calculation, the MMS can be used for control of the space station during the payload moving maneuvers. For such maneuvers, the inertias can change drastically. Instead of scheduling the controller gains at discrete intervals, the proposed MMS can be executed at the proper frequency so that the controller gains could be thought of as time-varying adaptive gains. For specific changes in the inertias, a new estimated TEA and set of gains can be computed. It is anticipated that these time-varying gains would stabilize the system because they will be based on the new linearized EOM presented in this paper.

Appendix: Linearized Equations

In this section the $\boldsymbol{A}$ and $\boldsymbol{B}$ matrices representing the linearized EOM about any arbitrary point are presented. Applying small perturbations to Eq. (1) will yield

$$\boldsymbol{I}\,\delta\dot{\omega} + (\tilde{\omega}\boldsymbol{I} - \boldsymbol{I}\omega)\,\delta\omega = \delta\boldsymbol{T}_{nc} + \delta\boldsymbol{u} \tag{A1}$$

Equations (4) and (5) are used to compute expressions for $\delta\omega$ and $\delta\dot{\omega}$:

$$\delta\omega = (\delta \boldsymbol{F})\dot{\Phi} + \boldsymbol{F}\delta\dot{\Phi} + \delta\boldsymbol{G} \tag{A2}$$

$$\delta\dot{\omega} = (\delta \boldsymbol{F})\ddot{\Phi} + \boldsymbol{F}\delta\ddot{\Phi} + (\delta\dot{\boldsymbol{F}})\dot{\Phi} + \dot{\boldsymbol{F}}\delta\dot{\Phi} + \delta\dot{\boldsymbol{G}} \tag{A3}$$

where

$$\delta\boldsymbol{F} = \frac{\partial \boldsymbol{F}}{\partial \Phi}\delta\Phi, \qquad \delta\dot{\boldsymbol{F}} = \frac{\partial \dot{\boldsymbol{F}}}{\partial \Phi}\delta\Phi + \frac{\partial \dot{\boldsymbol{F}}}{\partial \dot{\Phi}}\delta\dot{\Phi} \tag{A4}$$

$$\delta\boldsymbol{G} = \frac{\partial \boldsymbol{G}}{\partial \Phi}\delta\Phi, \qquad \delta\dot{\boldsymbol{G}} = \frac{\partial \dot{\boldsymbol{G}}}{\partial \Phi}\delta\Phi + \frac{\partial \dot{\boldsymbol{G}}}{\partial \dot{\Phi}}\delta\dot{\Phi} \tag{A5}$$

It is easily shown that

$$\partial\boldsymbol{G}/\partial\Phi = \partial\dot{\boldsymbol{G}}/\partial\dot{\Phi}$$

The term $\delta \boldsymbol{T}_{nc}$ is also provided as follows:

$$\delta\boldsymbol{T}_{nc} = 3n^2(\widetilde{\boldsymbol{R}}\boldsymbol{I} - \widetilde{\boldsymbol{IR}})\delta\boldsymbol{R} \tag{A6}$$

$$\delta\boldsymbol{T}_{\text{aero}} = 0 \qquad \text{and} \qquad \delta\boldsymbol{R} = \frac{\partial \boldsymbol{R}}{\partial \Phi}\delta\Phi \tag{A7}$$

Equations (A2) and (A3) can be further simplified by noting that $\dot{\Phi}$ and $\ddot{\Phi}$ vanish on the reference trajectory, implying that

$$\dot{\boldsymbol{F}} = 0, \qquad \dot{\boldsymbol{G}} = 0, \qquad \partial\dot{\boldsymbol{G}}/\partial\Phi = 0 \tag{A8}$$

and

$$\delta\omega = \boldsymbol{F}\delta\dot{\Phi} + \frac{\partial \boldsymbol{G}}{\partial \Phi}\delta\Phi \tag{A9}$$

$$\delta\dot{\omega} = \boldsymbol{F}\delta\ddot{\Phi} + \frac{\partial \boldsymbol{G}}{\partial \Phi}\delta\dot{\Phi} \tag{A10}$$

Equation (A10) is then solved to obtain the linearized EOM about any arbitrary point:

$$\delta\ddot{\Phi} = \boldsymbol{F}^{-1}\left(\delta\dot{\omega} - \frac{\partial \boldsymbol{G}}{\partial \Phi}\delta\dot{\Phi}\right) \tag{A11}$$

Finally, Eqs. (A9) and (A10) are used in Eq. (A11) to eliminate any dependence on the body angular rates:

$$\delta\ddot{\Phi} = (\boldsymbol{IF})^{-1}\left(3n^2(\widetilde{\boldsymbol{R}}\boldsymbol{I} - \widetilde{\boldsymbol{IR}})\frac{\partial \boldsymbol{R}}{\partial \Phi} - (\widetilde{\omega}\boldsymbol{I} - \widetilde{\boldsymbol{I}\omega})\frac{\partial \boldsymbol{G}}{\partial \Phi}\right)\delta\Phi - \left((\boldsymbol{IF})^{-1}(\widetilde{\omega}\boldsymbol{I} - \widetilde{\boldsymbol{I}\omega})\boldsymbol{F} + \boldsymbol{F}^{-1}\frac{\partial \boldsymbol{G}}{\partial \Phi}\right)\delta\dot{\Phi} + (\boldsymbol{IF})^{-1}\delta\boldsymbol{u} \tag{A12}$$

Note that the coefficients of $\delta\Phi$ and $\delta\dot{\Phi}$ are evaluated at the desired reference trajectory. These coefficients form the components of the $\boldsymbol{A}$ and $\boldsymbol{B}$ matrices, which are then complemented with CMG momentum, Eq. (14), and filter equations, Eqs. (16–18), in order to compute the system matrices for gain computation.

Acknowledgment

The author would like to thank Mendy Shapiro at Grumman for his guidance, support, and encouragement on this work.

References

[1]Hattis, P. D., "Predictive Momentum Management for the Space Station," *Journal of Guidance, Control, and Dynamics*, Vol. 9, No. 4, 1986, pp. 454-461.

[2]Bishop, L. R., Bishop, R. H., and Lindsay, K. L., "Proposed CMG Momentum Management Scheme for Space Station," *Proceedings of the AIAA Guidance, Navigation, and Control Conference* (Monterey, CA), AIAA, Washington, DC, 1987 (AIAA Paper 87-2528).

[3]Wie, B., Byun, K. W., Warren, W., Geller, D., Long, D., and Sunkel, J., "A New Momentum Management Controller for the Space Station," *Journal of Guidance, Control, and Dynamics*, Vol. 12, No. 5, 1989, pp. 714–722.

[4]Warren, W., Wie, B., and Geller, D., "Periodic-Disturbance Accommodating Control of the Space Station for Asymptotic Momentum Management," *Journal of Guidance, Control, and Dynamics*, Vol. 13, No. 6, 1990, pp. 984–992.

[5]Sunkel, J., and Shieh, L., "An Optimal Momentum Management Controller for the Space Station," *Journal of Guidance, Control, and Dynamics*, Vol. 13, No. 4, 1990, pp. 659–668.

[6]Woo, H. H., Morgan, H. D., and Falangas, E. T., "Momentum Management and Attitude Control Design for a Space Station," *Journal of Guidance, Control, and Dynamics*, Vol. 11, No. 1, 1988, pp. 19–25.

[7]Holmes, E., "The Limitations of the Linearization Techniques on Nonlinear Space Station Equations of Motion," Grumman Space Station Engineering Integration Contractor, Rept. No. PSH-341-RP89-002, Aug. 1989.

[8]Junkins, J. L., and Turner, J. D., "Optimal Spacecraft Rotational Maneuvers," *Studies in Astronautics 3*, Elsevier, New York, 1985.